

Article

Large Magnetic Entropy Change in GdRuSi Optimal for Magnetocaloric Liquefaction of Nitrogen

Anatoly G. Kuchin ¹, Sergey P. Platonov ¹, Roman D. Mukhachev ¹, Alexey V. Lukoyanov ^{1,2,*},
Aleksy S. Volegov ^{1,3}, Vasilii S. Gaviko ^{1,3} and Mari Yu. Yakovleva ¹

¹ M.N. Mikheev Institute of Metal Physics of Ural Branch of Russian Academy of Sciences, 620108 Ekaterinburg, Russia

² Institute of Physics and Technology, Ural Federal University Named after the First President of Russia B.N. Yeltsin, 620002 Ekaterinburg, Russia

³ Institute of Natural Sciences and Mathematics, Ural Federal University Named after the First President of Russia B.N. Yeltsin, 620026 Ekaterinburg, Russia

* Correspondence: lukoyanov@imp.uran.ru; Tel.: +7-3433783886

Abstract: The search for new magnetocaloric materials for application in magnetic refrigerants is highly motivated by high efficiency, reliability, and environmental safety. The values of the magnetocaloric effect MCE and the refrigerant capacity RC for the equiatomic GdRuSi compound were determined to be $MCE = 10.7$ and 4.94 J/kgK and $RC = 336$ and 92 J/kg with a change in the field of 0–50 and 0–17 kOe, respectively. These high values of MCE and RC for GdRuSi appear in the region of nitrogen liquefaction temperature of 77.4 K, due to which the compound can be useful in practice. The densities of states and magnetic moments of GdRuSi were calculated theoretically, taking into account strong electron correlations in the 4f Gd shell. The total magnetic moment of GdRuSi was found to be composed of the Gd moment only with the value calculated in very good agreement with the experimental one.

Keywords: magnetic measurements; magnetocaloric effect; electronic structure; intermetallics



Citation: Kuchin, A.G.; Platonov, S.P.; Mukhachev, R.D.; Lukoyanov, A.V.; Volegov, A.S.; Gaviko, V.S.; Yakovleva, M.Y. Large Magnetic Entropy Change in GdRuSi Optimal for Magnetocaloric Liquefaction of Nitrogen. *Metals* **2023**, *13*, 290. <https://doi.org/10.3390/met13020290>

Academic Editors: Changlong Tan, Kun Zhang and Yan Feng

Received: 30 December 2022

Revised: 26 January 2023

Accepted: 30 January 2023

Published: 31 January 2023



Copyright: © 2023 by the authors. Licensee MDPI, Basel, Switzerland. This article is an open access article distributed under the terms and conditions of the Creative Commons Attribution (CC BY) license (<https://creativecommons.org/licenses/by/4.0/>).

1. Introduction

Functional magnetic materials such as permanent or soft magnets, magnetostrictive, and magnetic shape memory compounds are very important for application in modern society. An urgent problem is the search for new magnetocaloric materials for magnetic refrigerates in view of high efficiency, reliability, and environmental safety [1–3]. The outstanding magnetocaloric performances have been reported on heavy rare earth-based compounds [1–5], MnTZ (T = Co and Fe; Z = Ge and Si)-based compounds [6], Ni-Mn-Y (Y = Ga, In and Sn)-based compounds [7], La(Fe, Si)₁₃H_x-based compounds [8], etc., with the MCE about 20–25 J/kgK in a field changing to 50 kOe. The temperature range in which MCE is pronounced is also important [1–4]. The so-called refrigerant capacity RC indicates how much heat can be transferred from the cold end to the hot end of a refrigerator in one refrigeration cycle. The giant-MCE materials have large MCE values extending over a narrow temperature range and irreversible character of MCE with a hysteresis due to the first-order phase transitions. Materials with the second-order phase transitions (the most used is Gd with $MCE = 9.8$ J/kgK at $T_C = 293$ K in a field changing to 50 kOe) present smaller MCE values spread over substantially a broader temperature range. It should be noted that the vast majority of the magnetocaloric materials exhibit large MCE values of the order of 10–30 J/kgK at cryogenic temperatures [9,10].

The ternary intermetallic RTX compounds (R = rare earth, T = transitional metal, X = p block metal) have attracted much attention, due to their interesting physical properties [9]. The RTX compounds have gained significant importance in power, electronics, and telecommunications industries because of their magnetic, electronic, and chem-

ical properties [9]. Recently, a ternary Gd-Ru-Si intermetallic compound with the close 122 composition attracted tremendous attention from researchers due to the nanometric square skyrmion lattice discovered in its centrosymmetric tetragonal lattice [11].

The GdFeSi and GdRuSi compounds crystallize in tetragonal structure of the CeFeSi type (space group $P4/nmm$) [12,13]. The hybridization between Si p states and 3d states of transition metal atom leads to the filling of 3d band and absence of the magnetic moment of Fe in the RFeSi compounds [12]. The GdFeSi and GdRuSi compounds are ferromagnetic below $T_C = 135$ and 85 K, respectively [12,13]. It was found that the GdFeSi compound exhibits a rather large value of the magnetocaloric effect MCE of 5 J/kgK [14,15] at $T_C = 130$ K [15] in a field changing to 17 kOe. This value is in line with the following new promising rare-earth-based compounds with a hysteresis-free second-order magnetic phase transition at about 100 K for use in magnetic refrigeration, such as DyFeSi with maximum magnetic entropy change (i.e., MCE) $-\Delta S_M = 9.2$ J/kgK at 70 K with the magnetic field change of 0–20 kOe [16], TbFeSi with $-\Delta S_M = 9.8$ J/kgK (0–20 kOe) at 110 K [16], Tb₃Co with $-\Delta S_M = 28.8$ J/kgK (0–70 kOe) at 84 K [17], Gd₂Cu₂Cd with $-\Delta S_M = 7.8$ J/kgK (0–50 kOe) at 120 K [18]. We can assume the same large value of the MCE in the case of GdRuSi as for GdFeSi, keeping in mind the close values of the MCE for ErRuSi (21.2 J/kgK) and ErFeSi (23.1 J/kgK) in a field changing to 50 kOe [9] and that only the R component is magnetic in RRuSi and RFeSi [9,12,13]. Considering the proximity of $T_C = 85$ K of GdRuSi [9] to the liquefaction of nitrogen temperature $T = 77.4$ K, it is of interest to study the magnetocaloric effect for GdRuSi.

2. Materials and Methods

The GdRuSi compound was prepared by arc melting in an argon atmosphere. The ingot was homogenized at 1273 K for 8 days and then quenched in water. X-ray powder diffraction analysis was employed to determine the phase composition, structure type, and lattice parameters under ambient conditions. A diffractometer of Empyrean Series 2 (PANalytical, Malvern, UK) and CuK α radiation was used. The HighScore v.4.x programs were employed for the calculation of lattice parameters and analysis of phase compositions. A vibromagnetometer 7407 VSM (Lake Shore Cryotronics, Westerville, OH, USA) and SQUID-magnetometer MPMS XL7 (Quantum Design, San Diego, CA, USA) were used for magnetic study in a magnetic field up to 7 T. The magnetization curves $M(H)$ were measured at 4 K on free powder samples previously oriented by an external field of 7 T upon cooling from room temperature. They were corrected by simple subtraction of the GdRu₂Si₂ impurity contribution. The temperature of the magnetic phase transition in the sample was determined from the magnetization vs. temperature $M(T)$ curves measured in a magnetic field of 0.01 T and in the temperature range 4–440 K. The T_C was also determined with the help of Arrott plots.

The first principles theoretical calculations of magnetic moments and electronic structure of the ternary GdRuSi compound were completed within the DFT+U method [19] in the Quantum ESPRESSO computational package [20,21] based on the exchange–correlation functional approximation in the form of generalized gradient approximation (GGA), version Perdew–Burke–Ernzerhof (PBE) [22]. For the sufficient convergence in our self-consistency cycle, an energy cutoff for plane waves equal to 60 Ry was set. Integration in reciprocal space was based on a grid of $12 \times 12 \times 12$ k -points. In the calculations, we used the projected augmented wave (PAW) datasets for Gd [23] and standard PAW pseudopotentials for Ru and Si from the pseudopotential library of Quantum ESPRESSO [24]. In 4f Gd shell, strong electron correlations were taken into account as the +U correction for direct Coulomb parameter equal to 6.7 eV and exchange parameter equal to 0.7 eV, which are commonly employed for Gd as a metal and in various Gd-based intermetallic compounds [19,25].

3. Results

3.1. Crystal Structure Analysis

The GdRuSi compound investigated crystallize into the tetragonal CeFeSi ($P4/nmm$)-type structure with the lattice parameters $a = 4.192 \text{ \AA}$ and $c = 6.602 \text{ \AA}$. These values are close to $a = 4.173(2) \text{ \AA}$ and $c = 6.586(4) \text{ \AA}$ found in [13]. The fraction of a parasitic antiferromagnetic GdRu₂Si₂ phase is also presented in the alloy, however the amount of dominant phase could be estimated as >95%. The experimental and calculated X-ray diffraction patterns for GdRuSi are shown in Figure 1. The presence of small additional reflections from GdRu₂Si₂ were taken into account in simulations.

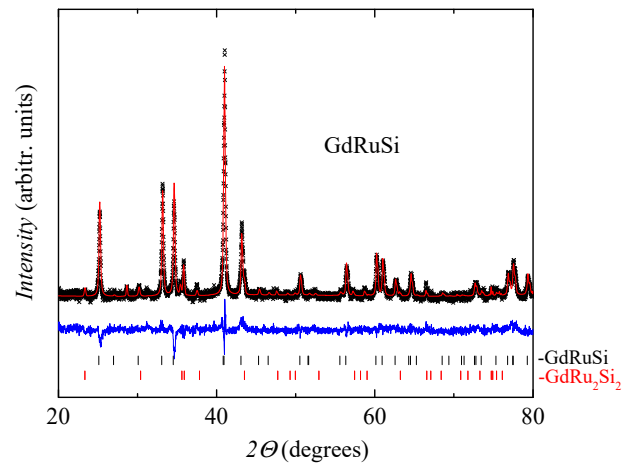


Figure 1. X-ray diffraction pattern (symbols) and its fitting (envelop line) of GdRuSi. The lower curve is the difference between the experimental and calculated results. Vertical lines show the reflection positions for the (up-down) GdRuSi and GdRu₂Si₂ compounds.

3.2. Magnetic Properties and Electronic Structure

Figure 2 shows the magnetization curves for the GdRuSi compound, which were measured at 4 K on free powder samples previously oriented along easy magnetization axis by an external field of 70 kOe upon cooling from room temperature. The magnetization curve is typical of ferro- or ferrimagnets, similarly to GdFeSi [25]. The GdRuSi compound has a saturation magnetization of the order of $7 \mu_B/\text{f.u.}$ (Figure 2), which equals to the value of the magnetic moment for a free Gd ion. This means it is a collinear ferromagnet. There is virtually no magnetic hysteresis on the $M(H)$ dependence for GdRuSi.

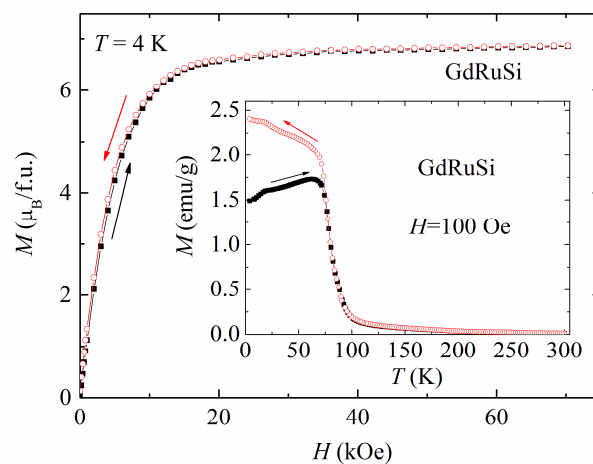


Figure 2. Magnetization and demagnetization curves of free powder sample of GdRuSi at $T = 4 \text{ K}$. The inset shows field-cooled (FC) and zero-field-cooled (ZFC) thermomagnetic curves of GdRuSi collected in an applied field of 100 Oe applied along easy magnetization axis of the free powder sample.

The zero-field-cooled thermomagnetic curve ZFC $M(T)$ for the GdRuSi compound measured in a field of 100 Oe on free powder sample previously oriented along easy magnetization axis by an external field of 70 kOe is presented in Figure 2. The increase in ZFC $M(T)$ upon heating from 4 K can be caused by domain-wall movement [26]. Such an increase in field-cooled FC $M(T)$ was not observed when cooling the sample in a field of 100 Oe (see Figure 2) because the maximum order degree for that magnetic field has already been reached [26]. There is no thermal hysteresis on the $M(T)$ dependence for GdRuSi in the region of the temperature of the magnetic phase transition of the ferro-paramagnet, i.e., this is a second-order phase transition. The Curie temperature $T_C = 78.3$ K of the alloys was determined from the position of the minimum of the derivative for the $M(T)$ dependence. Earlier in [13] a slightly larger value of $T_C = 85$ K was established, perhaps because of measurements in higher field up to 15 kOe, which creates an additional ordering effect on the magnetic moments of the ions. It is also seen (Figure 2) that there is a small jump at $T \sim 18$ K, presumably corresponding to the magnetic phase transition from antiferromagnetic to ferromagnetic ordering in the parasitic GdRu₂Si₂ phase [27]. The presence of this phase in the GdRuSi sample was established by X-ray diffraction (see Section 3.1). There are no other features on the $M(T)$ dependence caused by magnetic phase transformations in the GdRuSi sample.

The $T_C = 78.3$ K for GdRuSi was also determined with the help of Arrott plots [28] as is shown in Figure 3. The positive slope of the Arrott curves indicate that the ferromagnet-to-paramagnet transition can be classified as second-order type-phase transition according to the Banerjee criterion [28]. A similar conclusion follows from the absence of thermal hysteresis on the $M(T)$ dependence for GdRuSi in the region of the ferromagnet-to-paramagnet phase transition (Figure 2) and from the “caret” shape of the temperature dependence of the change in magnetic entropy $-\Delta S_M(T)$ (see Section 3.1), which is typical of the second-order magnetic-phase transition [28].

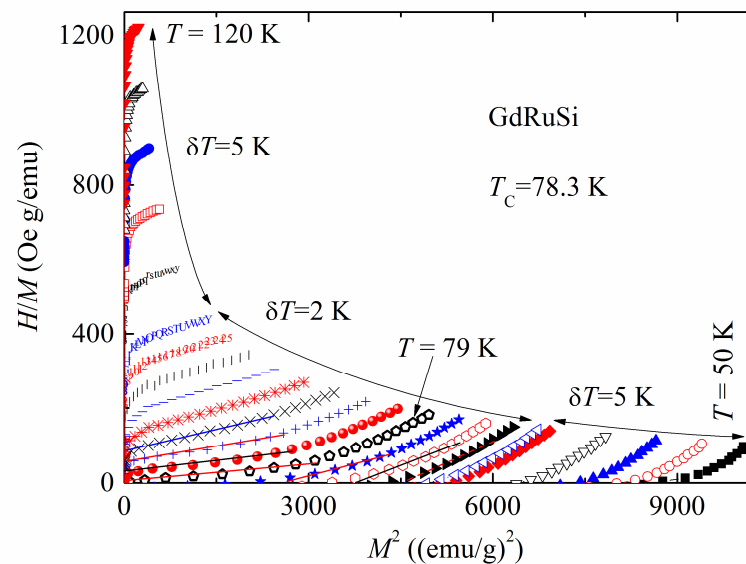


Figure 3. Arrott plots for the GdRuSi compound. Different colors for different symbols are made to better distinguish them.

The densities of electronic states for the GdRuSi compound are shown in Figure 4. The Fermi energy (E_F) is shown as a vertical dashed line at zero energy. The most intense DOS peaks (shown in red in Figure 4) near -6.5 and 5.8 eV are formed by the 4f localized electronic states of Gd. Due to the strong electron correlations in the 4f Gd shell taking into account in our GGA+U calculations, these peaks are shifted from the Fermi energy, because the 4f electronic states are half-filled. In the energy range from -4 eV up to 4 eV, the density of electronic states formed due to the 4d states of Ru and 3p states of Si. These electronic

states are almost spin unpolarized, i.e., almost the same for both spin projections. In the calculations, the ferromagnetic ordering of the Gd magnetic moments is found, whereas Ru and Si are converged to be nonmagnetic (less than $0.02 \mu_B$). Nonmagnetic 3d ions are also found in the calculations for similar Gd-based ternary intermetallics [25,29,30]. For example, in GdTiSi [29] or in the close compound GdNiGe [30], the Ti and Ni, as well as Si or Ge, are calculated to be nonmagnetic, correspondingly. Moreover, in GdFeSi, the electronic structure calculations also revealed that the iron ions are nonmagnetic, which is caused by the presence of silicon in GdFeSi [25]. For the Gd ions, the strong spin polarization at half-filling of the 4f shell results in the magnetic moment $7.1 \mu_B$ (per Gd ion and per f.u.), which is in very good agreement with the above experimental value $7 \mu_B/\text{f.u.}$, see above.

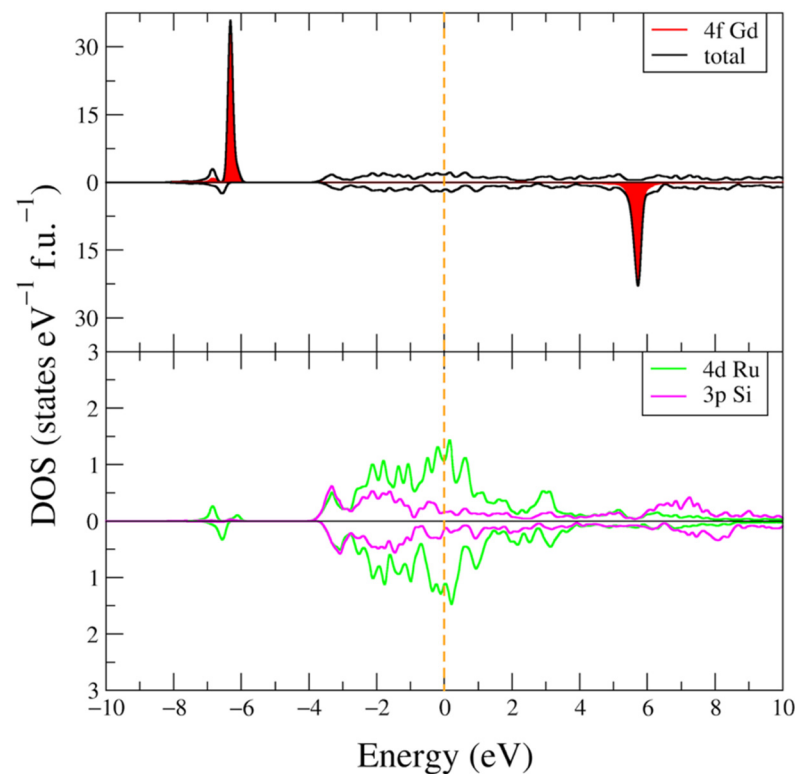


Figure 4. Calculated total (black curves) and partial densities of states of GdRuSi. The Fermi energy (E_F) is set at zero and shown as a vertical dashed orange line.

3.3. Magnetocaloric Effect

The isothermal magnetic entropy change $-\Delta S_M$ (i.e., the magnetocaloric effect MCE) was calculated from the magnetization isotherms $M(H)$ using the well-known Maxwell relation [9]:

$$\Delta S_M(T, H) = \int_0^H \left(\frac{\partial M}{\partial T} \right)_H dH \quad (1)$$

Magnetization isotherms $M(H)$ of GdRuSi in the range $T = 50$ – 120 K are shown in Figure 5. The temperature step is 5 K in the ranges 50–70, 95–120 K and 2 K in the range 71–95 K.

Figure 6 illustrates the isothermal magnetic entropy changes $-\Delta S_M$ (1) for GdRuSi as a function of temperature in a field changing to 10–50 kOe. Their “caret” shape is typical of the second-order magnetic-phase transition [28]. A similar conclusion follows from the form of the Arrott plots for GdRuSi (Figure 3) and from the absence of thermal hysteresis on the $M(T)$ dependence for GdRuSi in the region of the temperature of the ferromagnet-to-paramagnet phase transition (Figure 2).

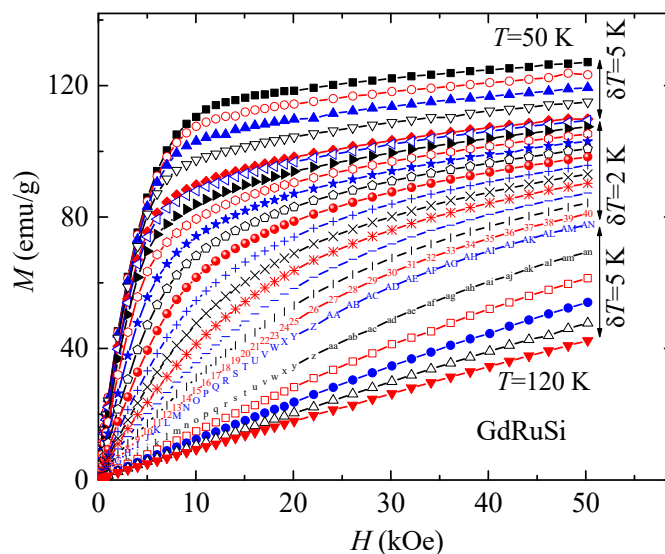


Figure 5. Magnetization isotherms $M(H)$ of GdRuSi in the range $T = 50\text{--}120$ K (up-down). The temperature step is 5 K in the ranges 50–70, 95–120 K and 2 K in the range 71–95 K. Different colors for different symbols are made to better distinguish them.

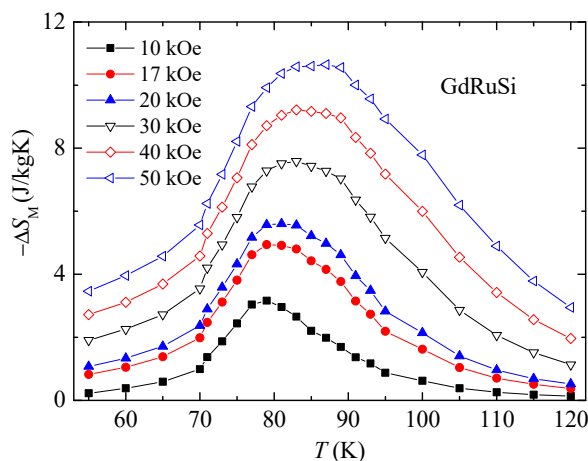


Figure 6. Temperature dependences of the change in magnetic entropy $-\Delta S_M(T)$ in a field changing to 10–50 kOe for GdRuSi.

For the GdRuSi equiatomic compound, a large value of the MCE was found, which is 10.7 at 87 K and 4.94 J/kgK at 79 K in a field change of 0–50 and 0–17 kOe, respectively. The value 4.94 J/kgK is somewhat less than 5 J/kgK for GdFeSi when the field changes 0–17 kOe [15]. At the same time, the Curie temperature T_C of GdFeSi equals to 130 K [15] and of GdRuSi—78.3 K, well below room temperature for practical application in domestic magnetic refrigerator. In this situation, successful alloying can be a good way to increase T_C of these compounds. For example, a sharp increase in T_C up to 184.4 K (by 54.4 K) was established when Ti atoms were substituted for Fe in the GdFe $_{1-x}$ Ti $_x$ Si compounds at $x = 0.1$ [15].

The value $-\Delta S_M(T_C) = 5.6$ J/kgK for GdRuSi (Figure 6) is noticeably smaller than $-\Delta S_M(T_C) = 9.2$ J/kgK for DyFeSi [10] in a field changing to 20 kOe. However, $T_C = 78.3$ K and, consequently, the $-\Delta S_M(T_C)$ maximum for GdRuSi are closer to the nitrogen liquefaction temperature of 77.4 K than $T_C = 70$ K for DyFeSi. Therefore, GdRuSi is more efficient for nitrogen liquefaction than DyFeSi.

The refrigerant capacity RC was estimated by numerical integration of the area under the $-\Delta S_M(T)$ curve between the temperatures T_1 and T_2 at the width of half maximum of the peak [14]:

$$RC = - \int_{T_1}^{T_2} \Delta S_M dT \quad (2)$$

The RC value of the GdRuSi compound equals to 336 J/kg (for $T_1 = 69$ K and $T_2 = 109$ K) and 92 J/kg (for $T_1 = 71$ K and $T_2 = 94$ K) in a field changing to 50 or 17 kOe, respectively.

The GdRuSi compound with large $-\Delta S_M(T_C) = 4.94$ J/kgK at $T_C = 78.3$ K and $RC = 92$ J/kg in a field changing to 1.7 T can be of practical interest due to T_C being close to nitrogen liquefaction temperature of 77.4 K.

4. Conclusions

The values of the magnetocaloric effect MCE and the refrigerant capacity RC for the equiatomic GdRuSi alloy were determined, which are MCE = 10.7 and 4.94 J/kgK and $RC = 336$ and 92 J/kg with a change in the field of 0–50 and 0–17 kOe, respectively. These large values of MCE and RC for GdRuSi with $T_C = 78.3$ K appear in the region of nitrogen liquefaction temperature of 77.4 K, due to which the compound can be useful in practice. The value of 4.94 J/kgK is quite large and almost coincides with the previously obtained 5 J/kgK at $T_C = 130$ K and a field change of 0–1.7 T for GdFeSi. In the calculated densities of states of GdRuSi, we identified the localized 4f Gd states, which required the accounting for electron correlations within DFT+U. The theoretical total magnetic moment of GdRuSi was found to be solely formed by the Gd ion (the Ru and Si ions were calculated to be nonmagnetic similar to Fe and Si in the previously considered ternary GdFeSi intermetallic compound), and its value is in very good agreement with the experimental data. Further search of magnetocaloric materials among gadolinium compounds may result in the discovery of novel materials useful for various environmentally sustainable applications.

Author Contributions: Conceptualization; methodology, A.G.K. and A.V.L.; software, R.D.M. and A.V.L.; validation, A.G.K. and A.V.L.; investigation, S.P.P., R.D.M., A.V.L., A.S.V. and V.S.G.; formal analysis, V.S.G. and S.P.P.; data curation; visualization, M.Y.Y.; writing—original draft preparation; writing—review and editing, A.G.K. and A.V.L.; supervision, A.G.K. and A.V.L.; project administration, A.V.L. All authors have read and agreed to the published version of the manuscript.

Funding: The results of Sections 1, 2, 3.1 and 3.2 (magnetic properties and electronic structure calculations) were obtained within the grant of the Russian Science Foundation No. 18-72-10098, <https://rscf.ru/en/project/18-72-10098/> (accessed on 29 December 2022). The results of Section 3.3 were obtained within the state assignment of Ministry of Science and Higher Education of the Russian Federation (themes “Magnet” No. 122021000034-9 and “Electron” No. 122021000039-4).

Institutional Review Board Statement: Not applicable.

Informed Consent Statement: Not applicable.

Data Availability Statement: The data presented in this study are available on request from the corresponding author.

Acknowledgments: X-ray diffraction and magnetometric measurements were conducted on equipment of the Collaborative Access Center “Testing Center of Nanotechnologies and Advanced Materials” of the Institute of Metal Physics (Ural Branch, Russian Academy of Sciences).

Conflicts of Interest: The authors declare no conflict of interest. The funders had no role in the design of the study; in the collection, analyses, or interpretation of data; in the writing of the manuscript, or in the decision to publish the results.

References

1. Li, L.; Yan, M. Recent progresses in exploring the rare earth based intermetallic compounds for cryogenic magnetic refrigeration. *J. Alloys Compd.* **2020**, *823*, 153810. [[CrossRef](#)]
2. Franco, V.; Blázquez, J.S.; Ipus, J.J.; Law, J.Y.; Moreno-Ramírez, L.M.; Conde, A. Magnetocaloric effect: From materials research to refrigeration devices. *Prog. Mater. Sci.* **2018**, *93*, 112–232. [[CrossRef](#)]
3. Takeuchi, I.; Sandemana, K. Solid-state cooling with caloric materials. *Phys. Today* **2015**, *68*, 48–54. [[CrossRef](#)]
4. Li, L. Review of magnetic properties and magnetocaloric effect in the intermetallic compounds of rare earth with low boiling point metals. *Chin. Phys.* **2016**, *25*, 037502. [[CrossRef](#)]
5. Zhang, Y. Review of the structural, magnetic and magnetocaloric properties in ternary rare earth RE₂T₂X type intermetallic compounds. *J. Alloys Compd.* **2019**, *787*, 1173–1186. [[CrossRef](#)]
6. Li, Y.; Zeng, Q.; Wei, Q.; Liu, E.; Han, X.; Du, Z.; Li, L.; Xi, X.; Wang, W.; Wang, S.; et al. An efficient scheme to tailor the magnetostructural transitions by staged quenching and cyclical ageing in hexagonal martensitic compounds. *Acta Mater.* **2019**, *174*, 289–299. [[CrossRef](#)]
7. Qu, Y.; Cong, D.; Li, S.; Gui, W.; Nie, Z.; Zhang, M.; Ren, Y.; Wang, Y. Simultaneously achieved large reversible elastocaloric and magnetocaloric effects and their coupling in a magnetic shape memory compound. *Acta Mater.* **2018**, *151*, 41–55. [[CrossRef](#)]
8. Ouyang, Y.; Zhang, M.; Yan, A.; Wang, W.; Guillou, W.; Liu, J. Plastically deformed La-Fe-Si: Microstructural evolution, magnetocaloric effect and anisotropic thermal conductivity. *Acta Mater.* **2020**, *187*, 1. [[CrossRef](#)]
9. Gupta, S.; Suresh, K. Review on magnetic and related properties of RTX compounds. *J. Alloys Compd.* **2015**, *618*, 562–606. [[CrossRef](#)]
10. Zhang, H.; Shen, B. Magnetocaloric effects in RTX intermetallic compounds (R = Gd–Tm, T = Fe–Cu and Pd, X = Al and Si). *Chin. Phys.* **2015**, *24*, 127504. [[CrossRef](#)]
11. Duy Khanh, N.; Nakajima, T.; Yu, X.; Gao, S.; Shibata, K.; Hirschberger, M.; Yamasaki, Y.; Sagayama, H.; Nakao, H.; Peng, L.; et al. Nanometric square skyrmion lattice in a centrosymmetric tetragonal magnet. *Nat. Nanotechnol.* **2020**, *15*, 444–449. [[CrossRef](#)] [[PubMed](#)]
12. Welter, R.; Venturini, G.; Malaman, B. Magnetic properties of RFeSi (R≡La–Sm, Gd–Dy) from susceptibility measurements and neutron diffraction studies. *J. Alloys Compd.* **1992**, *189*, 49–58. [[CrossRef](#)]
13. Welter, R.; Venturini, G.; Malaman, B.; Ressouche, E. Crystallographic data and magnetic properties of new RTX compounds (R=La–Sm, Gd; T=Ru, Os; X=Si, Ge). Magnetic structure of NdRuSi. *J. Alloys Compd.* **1993**, *202*, 165–172. [[CrossRef](#)]
14. Włodarczyk, P.; Hawelek, L.; Zackiewicz, P.; Roy, T.; Chrobak, A.; Kaminska, M.; Kolano-Burian, A.; Szade, J. Characterization of magnetocaloric effect, magnetic ordering and electronic structure in the GdFe_{1-x}Co_xSi intermetallic compounds. *Mater. Chem. Phys.* **2015**, *162*, 273–278. [[CrossRef](#)]
15. Kuchin, A.; Platonov, S.; Gaviko, V.; Yakovleva, M. Magnetic and Structural Properties of GdFe_{1-x}Ti_xSi. *IEEE Magn. Lett.* **2019**, *10*, 2509204. [[CrossRef](#)]
16. Zhang, H.; Sun, Y.J.; Niu, E.; Yang, L.H.; Shen, J.; Hu, F.X.; Sun, J.R.; Shen, B.G. Large magnetocaloric effects of RFeSi (R=Tb and Dy) compounds for magnetic refrigeration in nitrogen and natural gas liquefaction. *Appl. Phys. Lett.* **2013**, *103*, 202412. [[CrossRef](#)]
17. Guzik, A.; Talik, E.; Zajdel, P. Magnetocaloric effect of the Gd_{3-x}Tb_xCo system. *Intermetallics* **2020**, *118*, 106686. [[CrossRef](#)]
18. Yang, Y.; Zhang, Y.K.; Xu, X.; Geng, S.H.; Hou, L.; Li, X.; Ren, Z.M.; Wilde, G. Magnetic and magnetocaloric properties of the ternary cadmium based intermetallic compounds of Gd₂Cu₂Cd and Er₂Cu₂Cd. *J. Alloys Compd.* **2017**, *692*, 665–669. [[CrossRef](#)]
19. Anisimov, V.I.; Aryasetiawan, F.; Lichtenstein, A.I. First-principles calculations of the electronic structure and spectra of strongly correlated systems: The LDA+U method. *J. Phys. Condens. Matter* **1997**, *9*, 767–808. [[CrossRef](#)]
20. Giannozzi, P.; Andreussi, O.; Brumme, T.; Bunau, O.; Buongiorno Nardelli, M.; Calandra, M.; Car, R.; Cavazzoni, C.; Ceresoli, D.; Cococcioni, M.; et al. Advanced capabilities for materials modelling with Quantum ESPRESSO. *J. Phys. Condens. Matter* **2017**, *29*, 465901. [[CrossRef](#)]
21. Giannozzi, P.; Baroni, S.; Bonini, N.; Calandra, M.; Car, R.; Cavazzoni, C.; Ceresoli, D.; Chiarotti, G.L.; Cococcioni, M.; Dabo, I.; et al. Quantum ESPRESSO: A modular and open-source software project for Quantum simulations of materials. *J. Phys. Condens. Matter* **2009**, *21*, 395502. [[CrossRef](#)]
22. Perdew, J.P.; Burke, J.P.; Ernzerhof, M. Generalized gradient approximation made simple. *Phys. Rev. Lett.* **1996**, *77*, 3865–3868. [[CrossRef](#)]
23. Topsakal, M.; Wentzcovitch, R. Accurate projected augmented wave (PAW) datasets for rare-earth elements (RE = La–Lu). *Comput. Mater. Sci.* **2014**, *95*, 263–270. [[CrossRef](#)]
24. Quantum ESPRESSO, Pseudopotentials. Available online: <https://www.quantum-espresso.org/pseudopotentials> (accessed on 29 December 2022).
25. Kuchin, A.G.; Platonov, S.P.; Lukoyanov, A.V.; Volegov, A.S.; Gaviko, V.S.; Mukhachev, R.D.; Yakovleva, M.Y. Remarkable increase of Curie temperature in doped GdFeSi compound. *Intermetallics* **2021**, *133*, 107183. [[CrossRef](#)]
26. Napoletano, M.; Canepa, F.; Manfrinetti, P.; Merlo, F. Magnetic properties and the magnetocaloric effect in the intermetallic compound GdFeSi. *J. Mater. Chem.* **2000**, *10*, 1663–1665. [[CrossRef](#)]
27. Ślaski, M.; Szytuła, A.; Leciejewicz, J.; Zygunt, A. Magnetic properties of RERu₂Si₂ (RE = Pr, Nd, Gd, Tb, Dy, Er) intermetallics. *J. Magn. Magn. Mater.* **1984**, *46*, 114–122. [[CrossRef](#)]

28. Gebara, P.; Hasiak, M. Determination of Phase Transition and Critical Behavior of the As-Cast GdGeSi-(X) Type Alloys (Where X = Ni, Nd and Pr). *Materials* **2021**, *14*, 185. [[CrossRef](#)] [[PubMed](#)]
29. Mukhachev, R.D.; Lukoyanov, A.V. Composition-Induced Magnetic Transition in GdMn_{1-x}Ti_xSi Intermetallic Compounds for x = 0–1. *Metals* **2021**, *11*, 1296. [[CrossRef](#)]
30. Baglasov, E.D.; Lukoyanov, A.V. Electronic Structure of Intermetallic Antiferromagnet GdNiGe. *Symmetry* **2019**, *11*, 737. [[CrossRef](#)]

Disclaimer/Publisher's Note: The statements, opinions and data contained in all publications are solely those of the individual author(s) and contributor(s) and not of MDPI and/or the editor(s). MDPI and/or the editor(s) disclaim responsibility for any injury to people or property resulting from any ideas, methods, instructions or products referred to in the content.